The EMBO Journal vol.13 no.10 pp.2441 – 2451, 1994

RNA 3′ end signals of the *S.pombe ura4* gene comprise a site determining and efficiency element

Tim Humphrey[1], Charles E.Birse and Nick J.Proudfoot[2]

Sir William Dunn School of Pathology, Oxford University, South Parks Road, Oxford, OX1 3RE, UK and [1]Department of Genetics, Harvard Medical School, 200 Longwood Ave, Boston, MA 02115, USA

[2]Corresponding author

Communicated by N.J.Proudfoot

We have defined sequences in the 3′ non-coding region of the *Schizosaccharomyces pombe ura4* gene that are required for efficient mRNA 3′ end formation. Three separate sequence elements have been identified. Two of these are site determining elements which specify alternative sites of polyadenylation [the major poly(A) site and a minor downstream poly(A) site]. The third sequence, located downstream of both poly(A) sites, functions as an efficiency element that enhances utilization of either polyadenylation site. By employing sensitive RT-PCR analysis, we demonstrate that although low levels of transcripts are detected up to the efficiency element, none is detected beyond this point. The downstream site determining element and efficiency element have both been delineated to specific 16 nt sequences which we show are together sufficient for *ura4* mRNA 3′ end formation. We have further characterized the interaction between these two elements and show that the efficiency element behaves in a position-independent, orientation-dependent manner, but cannot form 3′ ends independently of the site determining element. Surprisingly, we find that the efficiency element can be functionally replaced by a second copy of either site determining element. We present a model for the mechanism of RNA 3′ end formation of the *ura4* gene and note that this bipartite structure for a poly(A) signal in *S.pombe* may be related to the AAUAAA and downstream GU-rich sequences of poly(A) signals in mammalian genes.

Key words: 3′ end formation/mRNA/polyadenylation/*Schizosaccharomyces pombe/ura4*

Introduction

Messenger RNA 3′ end formation in yeast has been proposed to result from the coupled events of transcriptional termination and endonucleolytic cleavage followed by polyadenylation. A variety of assays have defined the signals required for these processes in the iso-1-cytochrome C (*CYC1*) gene of *Saccharomyces cerevisiae* . A 38 bp deletion in the 3′ non-coding region of *CYC1* (mutation *cyc1-512*) results in reduced levels of transcripts but with increased lengths, suggesting that transcriptional termination was defective (Zaret and Sherman, 1982). Furthermore, insertion of the 3′ non-coding region of the *CYC1* gene between the *GAL1* promoter and a *CEN3* element prevents plasmid instability caused by transcription into the centromeric element. The *cyc1-512* mutation loses this protective effect (Russo and Sherman, 1989). When an 83 bp fragment encoding this region of *CYC1* is present on a plasmid it halts RNA polymerase II, as determined by a decrease in negative supercoiling, otherwise caused by transcription (Osborne and Guarente, 1988) and by nuclear 'run-off' analysis (Osborne and Guarente, 1989). In addition, insertion of this 83 bp *CYC1* fragment into an intron located at the 5′ end of a gene fusion construct, leads to a reduction in the expression of the distal gene (Ruohola *et al.*, 1988; Hyman *et al.*, 1991).

Better understanding of transcriptional termination in yeast has recently been facilitated by the development of *in vitro* systems, where termination and pausing of RNA polymerase II has been detected downstream of polyadenylation sites *in vitro* (Hyman and Moore, 1993). Also, the *Escherichia coli* rho protein has been implicated in transcriptional arrest of yeast RNA polymerase II *in vitro* (Wu and Platt, 1993). Both of these findings are consistent with the model in which signals for transcriptional termination comprise a poly(A) site coupled with a pause site (Proudfoot, 1989). That pre-mRNA processing also plays a role in yeast mRNA 3′ end formation was first demonstrated by Butler and Platt (1988). They showed that mature polyadenylated 3′ ends were generated by incubating synthetic pre-mRNA made from the 3′ untranslated region of the same *CYC1* gene in whole cell extracts of *S.cerevisiae*. This *in vitro* process was also dependent on the 38 bp element, as synthetic pre-mRNA made from the 3′ non-coding region of *cyc1-512* was not processed. Taken together, these data suggest that transcriptional termination occurs close to the site of polyadenylation and that sequence elements within the 38 bp deletion are necessary for both transcriptional termination and pre-mRNA processing. A number of synthetically generated pre-mRNAs have subsequently been demonstrated to cleave accurately and efficiently and polyadenylate *in vitro* (Abe *et al.*, 1990; Butler *et al.*, 1990; Sadhale *et al.*, 1991). Also components involved in this process have recently been characterized. The poly(A) polymerase from *S.cerevisiae* has been purified (Lingner *et al.*, 1991a) and cloned (Lingner *et al.*, 1991b), and at least three other functionally distinct fractions are required for cleavage and polyadenylation of yeast precursor RNA (Chen and Moore, 1992).

Further studies have been performed to determine the sequence requirements for yeast mRNA 3′ end formation. Analysis of the sequences of the extended transcripts of *cyc1-512* revealed an homology UAG...UAGU...UUU, also found within the 38 bp deleted in *cyc1-512*. (Zaret and Sherman, 1982, 1984). However, a linker substitution study across the 83 bp fragment encoding this region of *CYC1*, which halts RNA polymerase II, shows that no single linker

substitution abolishes the transcriptional termination activity of the *CYC1* fragment (Osborne and Guarente, 1989). Russo *et al.* (1991), studying intragenic revertants of *cyc1-512* in which the mRNA deficiency was restored, found that revertants reform either TAG...TATGTA or TATATA/TACATA sequences and enhance the use of downstream preferred sites. This suggests that production of 3′ termini of yeast mRNA may involve at least two functionally distinct elements working in concert. Recently, Russo *et al.* (1993) have carried out further extensive analysis of the RNA 3′ end forming signals of *CYC1*. Their results show that the previously defined signals are required for efficient 3′ end formation, while additional downstream sequences ~20 nt upstream of the site of polyadenylation are involved in poly(A) site selection. A variety of different sequence elements have been implicated in yeast mRNA 3′ end formation for a number of other genes. The sequence TTTTTATA downstream of a *Drosophila* gene which complements a yeast *ade8* mutation was shown to be important for mRNA 3′ end formation (Henikoff *et al.*, 1983). Abe *et al.* (1990) describe an AT-rich 26 nt sequence required for mRNA 3′ end generation in the *S.cerevisiae GAL7* gene and show that this signal functions in an orientation-dependent fashion. Hyman *et al.* (1991) demonstrate that the sequence AATAAA, required for mammalian mRNA 3′ end formation (Proudfoot, 1991) and present at mRNA 3′ ends in 50% of yeast genes, is not required for 3′ end formation of the *ADH2* gene. Instead, point mutations reveal sequences 80 nt upstream of the *ADH2* poly(A) site to be important. Sadhale and Platt (1992) were unable to find common features for *in vitro* processing between *GAL7* and *CYC1* and instead, suggest that signals more widely dispersed than the polyadenylation site may be required. A study of the *ACT1*, *ADH1*, *CYC1* and *YPT1* cDNAs from *S.cerevisiae* demonstrates that the sites of polyadenylation *in vivo* can be scattered across a 200 nt region, suggesting a single signal sequence to be unlikely. However, a PyAAA sequence is essential for polyadenylation site selection of the *ADH1* gene from *S.cerevisiae* (Heidmann *et al.*, 1992). These disparate results may be reconciled to some extent by the proposal that different classes of polyadenylation sites may exist in *S.cerevisiae* (Irniger *et al.*, 1991),

A study of mRNA 3′ end formation in the distantly related fission yeast, *Schizosaccharomyces pombe*, demonstrates that in contrast to those of higher eukaryotes, 3′ untranslated regions of genes from both *S.cerevisiae* and *S.pombe* can be functionally interchanged. Furthermore, sequences within the 38 bp of the *CYC1* gene, deleted in *cyc1-512*, were required to form mRNA 3′ termini in both yeasts, suggesting an evolutionary conserved lower eukaryotic sequence requirement for mRNA 3′ end formation (Humphrey *et al.*, 1991). Although no components involved in 3′ end formation have been isolated from fission yeast, it has been demonstrated that polyadenylation of several *S.pombe* genes (*fib*, *gar2*, *ura4* and *cdc25*) is highly sensitive to cold shock as lowering the temperature appears to reduce usage of the normal site and increase polyadenylation at more distal locations (Girard *et al.*, 1993).

Here, we describe the definition of sequences required for RNA 3′ end formation in the *ura4* gene of *S.pombe*. We firstly define the extent of detectable transcripts beyond the major poly(A) site of the gene. We then demonstrate that

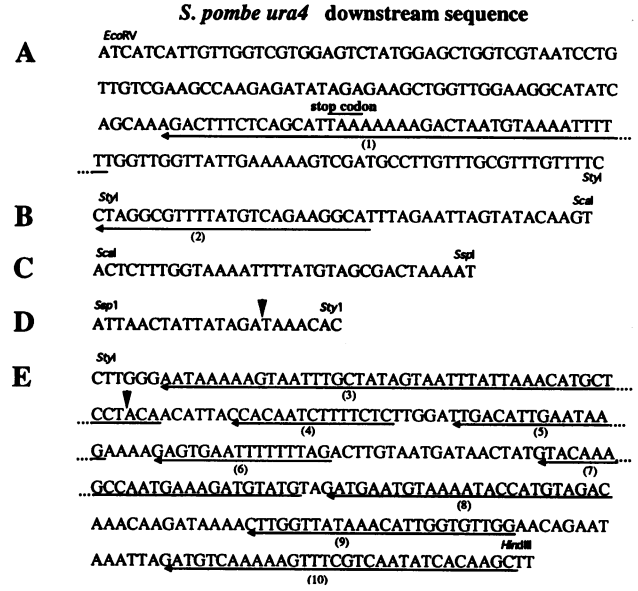

Fig. 1. Sequences of the five restriction fragments for the downstream region of the *S.pombe ura4* gene. A (*Eco*RV−*Sty*I), B (*Sty*I−*Sca*I), C (*Sca*I−*Ssp*I), D (*Ssp*I−*Sty*I) and E (*Sty*I−*Hin*dIII). The major *ura4* mRNA polyadenylation site is located in fragment D (indicated by a black arrow). A second polyadenylation site located in fragment E is also indicated. Arrows underlying *ura4* sequences represent positions of antisense oligonucleotides used in the RT-PCR assay in Figure 2.

within this transcribed portion of the *ura4* gene's 3′ flanking sequence there exists two types of sequence element required for RNA 3′ end formation. The first element determines the site of polyadenylation of the pre-mRNA transcript (called a site determining element). The second element enhances the efficiency of polyadenylation (called an efficiency element). We further demonstrate the relationship between these two elements and find that two site determining elements are also sufficient for efficient mRNA 3′ end formation.

Results

Detection of transcripts downstream of the ura4 gene

mRNA 3′ end formation in *S.cerevisiae* has been proposed to result from coupled transcriptional termination and pre-mRNA processing events. We therefore began our analysis of the RNA 3′ end formation signals of the *S.pombe ura4* gene by defining the site at which no further *ura4* transcripts can be detected in the 3′ flanking region of the gene. To obtain this information, *ura4* transcripts were analysed by the highly sensitive RT-PCR technique. DNA primers were hybridized to *ura4* RNA and the reverse transcribed cDNA products were then amplified using PCR.

The 551 nt region sequenced downstream of the *ura4* stop codon (Grimm *et al.*, 1988) can be conveniently divided into a series of restriction fragments, A−E. The sequence of each fragment is illustrated in Figure 1. Antisense oligonucleotides (the positions of oligonucleotides 1−10 are illustrated in Figures 1 and 2A) which span the downstream region of the *ura4* gene were used as primers for reverse transcription of DNase treated total RNA which was isolated from *S.pombe* transformed with PUS A−E (Figure 3B).

These reverse transcripts were PCR amplified using the same RT oligonucleotide and a common 5′ oligonucleotide which had been radioactively labelled. A linear relationship

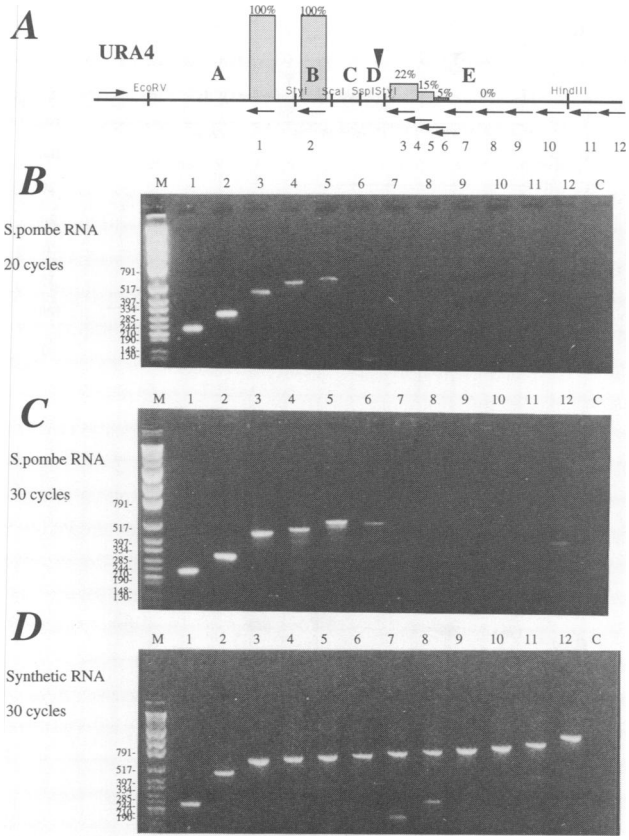

Fig. 2. Detection of transcripts downstream of the *ura4* gene. (**A**) A schematic representation of the relative positions of each oligonucleotide used for RT-PCR analysis with respect to the downstream region of the *S.pombe ura4* gene. The numbers of each oligonucleotide correspond to those shown in Figure 1. The relative ratios of RT-PCR products detected across the downstream non-coding region of the *S.pombe ura4* gene are shown above the appropriate oligonucleotide. (**B**) Electrophoretic separation of RT-PCR products generated by 20 PCR amplification cycles, using total RNA isolated from *S.pombe* transformed with PUS A−E, encoding an intact *ura4* gene. The RT-PCR products were separated on a 2% agarose gel. The lane numbers correspond to the 3′ oligonucleotide used for reverse transcription and PCR amplification. Lane C (control) has no RNA added to the RT-PCR assay. A common end-labelled 5′ oligonucleotide was used for each PCR. Radioactive PCR products were excised and quantitated. The radioactivity of each PCR product is given as a percentage of that recorded for the PCR product produced with oligonucleotide 1. The sizes of the DNA markers are also indicated. (**C**) Electrophoretic separation of RT-PCR products generated by 30 PCR amplification cycles, from total RNA isolated from *S.pombe* transformed with PUS A−E, encoding an intact *ura4* gene. The RT-PCR products were separated on a 2% agarose gel. The lane numbers correspond to the 3′ oligonucleotide used for reverse transcription and PCR amplification. Lane C (control) has no RNA added to the RT-PCR assay. The smaller PCR band in lane 12 is a PCR artefact. (**D**) Electrophoretic separation of RT-PCR products generated by 30 PCR amplification cycles, from synthetic *ura4* RNA generated by T7 polymerase. The RT-PCR products were separated on a 2% agarose gel. The lane numbers correspond to the 3′ oligonucleotide used for reverse transcription and PCR amplification. The synthetic RNA, which has a 130 nt spacer sequence in the *Avr*II site is otherwise identical to the *ura4* downstream non-coding sequence. Lane C (control) has no RNA added to the RT-PCR assay. The lower bands visible in lanes 7 and 8 are PCR artefacts.

between RNA input and PCR product was determined, as described in Owczarek *et al.* (1992) and was found to exist after 20 cycles of amplification, for 50 ng of *S.pombe* RNA (data not shown). Therefore a measure of the relative number of transcripts was made by comparing the counts incorporated into the PCR products separated electrophoretically (Figure 2B) after 20 cycles and is presented in Figure 2A. As a control of the RT-PCR efficiency for each pair of primers, a synthetic pre-mRNA was generated and similarly assayed (Figure 2D).

From such RT-PCR analysis, transcripts were detected past the previously mapped poly(A) site (Figure 2B and C, lanes 3−6), although at a much reduced level compared with the levels of transcripts detected upstream of the poly(A) site (Figure 2B, lanes 1 and 2). No RT-PCR products were detected after oligo 6 in region E, even after 30 cycles of amplification (compare Figure 2C, lanes 6 and 7) which should theoretically allow detection of a single transcript. This was confirmed by quantitating the radioactivity levels of this region of the gel (not shown). It is of particular interest that oligo 6 corresponds to sequence immediately upstream of the efficiency element described below. It would therefore appear that transcriptional termination occurs close to the most distal RNA 3′ end formation element defined in these studies. These observations may implicate signals within this region as having a role in transcriptional termination.

Sequences required for mRNA 3′ end formation in the S.pombe ura4 gene

We wished to determine which sequences are involved in mRNA 3′ end formation of the *S.pombe ura4* gene. Fragments A−E from the 3′ end of the *ura4* gene (Figure 1) were cloned into the *Bam*HI site of the plasmid PUS either separately or in combination (Figure 3A). This plasmid contains a truncated form of the *ura4* gene that lacks these 3′ sequences. A crude 5′ and 3′ deletion series was effectively constructed as shown in Figure 3B. These constructs were transformed into *S.pombe (ade6-704, ura4-d18, leu1-32, h⁺)* as previously described (Humphrey *et al.*, 1991) and mRNA 3′ end formation was determined by comparing the lengths of the subsequent *ura4* transcripts from these constructs using Northern blot analysis.

Insertion of the 551 nt *ura4* A−E fragment into the PUS construct (PUS A−E) results in *ura4* transcripts of ~1.0 kb in length (Figure 3C, lane 1). The *ura4* transcripts from this construct are similar in length to mRNA produced by the genomic *ura4* gene in wild-type *S.pombe* (h^-;972) as shown in Figure 3C (lanes 8 and 9). When the 284 bp *ura4* A−D fragment is inserted into the PUS construct (PUS A−D) only a minority (20%) of the *ura4* transcripts generated is of a length similar to those of PUS A−E (compare Figure 3C, lanes 1 and 2). The 3′ termini of *ura4* transcripts of ~1.0 kb in length appear to map to sites within fragment D. However, ~80% of the transcripts are 1.4 kb in length and are too long for 3′ termini to map within fragment A−D. These transcripts form 3′ termini at a cryptic site(s) within the downstream *LEU2* gene of PUS. These results imply that fragment A−D encodes sequences which direct 3′ end formation in only 20% of the *ura4* transcripts. Maximal efficiency of mRNA 3′ end formation requires the presence of fragment E, indicating that this downstream sequence plays an important role in 3′ end formation of *ura4* mRNA.

Insertion of the 260 bp *ura4* E fragment into the PUS construct (PUS E) results in *ura4* transcripts of ~750 nt in length (Figure 3C, lane 6). The 3′ termini of these transcripts map to a site within the 5′ end of fragment E (see later). As no larger readthrough transcripts are detected,

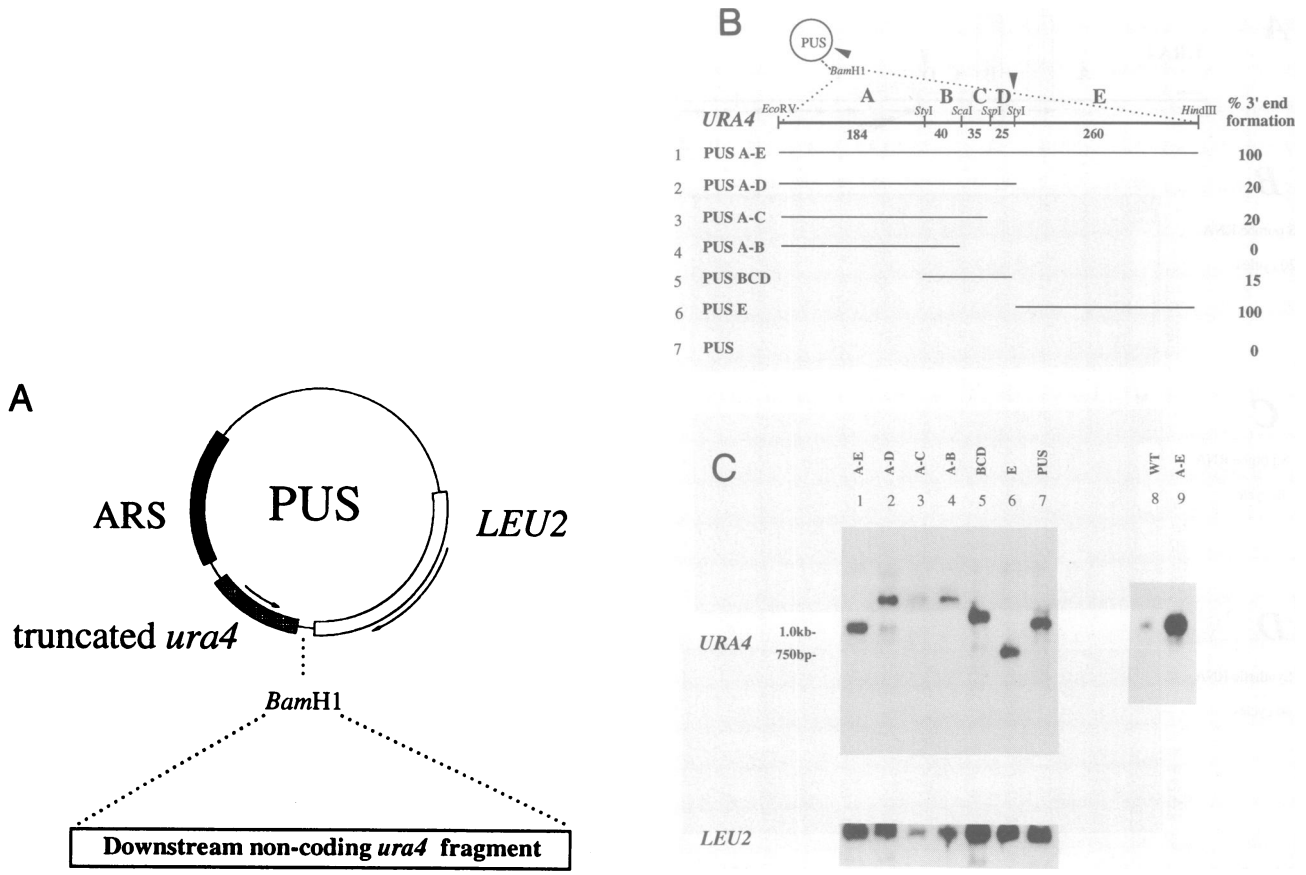

Fig. 3. Sequences required for mRNA 3′ end formation in the *S.pombe ura4* gene. (**A**) A diagram of plasmid PUS, constructed as previously described (Humphrey *et al.*, 1991). This encodes the *Hin*dIII−*Eco*RV fragment of the *S.pombe ura4* gene inserted into the *Sma*I site of Pirt2. Plasmid PUL has a 35 bp polylinker cloned into the *Bam*HI site of PUS. (**B**) A diagram of constructs transformed into *S.pombe*. The sizes of the various restriction endonuclease fragments are indicated. The major polyadenylation site located within fragment D is shown by a black arrow. An estimation of the ability of each fragment to form *ura4* mRNA 3′ ends is also shown. (**C**) Northern hybridization of total RNA isolated from *S.pombe* transformed with the constructs illustrated above. The RNA was separated on a 1.5% denaturing formaldehyde−agarose gel, transferred to a nylon membrane and hybridized to a 1.2 kb *Hin*cII−*Eco*RV random primer labelled DNA fragment of *ura4* to determine transcript lengths, which were compared with ethidium bromide stained RNA markers run in an adjacent lane. The larger RNA bands detected in lanes 2−5 reflect readthrough transcripts to cryptic poly(A) sites in the *LEU2* gene. The expression of *ura4* transcripts from the multicopy PUS plasmids is at a higher level than the endogenous *ura4* gene (lanes 8 and 9). The filter was stripped and rehybridized to a DNA 2.2 kb *Hin*dIII fragment from *S.cerevisiae LEU2* gene present on PUS, in order to standardize the amount of loaded RNA. The nomenclature of each lane corresponds to the constructs named in Figure 2B.

fragment E alone encodes signals which are efficiently recognized by mRNA 3′ end formation machinery in *S.pombe*. In contrast to fragment E, fragments ABC and BCD form 3′ ends inefficiently (see Figure 3C, lanes 3 and 5). Fragment AB cannot form 3′ ends alone and only extended readthrough transcripts are observed (Figure 3C, lane 4). The lower levels of *ura4* transcripts observed with PUS ABC and PUS AB correspond to lower levels of *LEU2* mRNA as shown in the bottom panel (presumably resulting from unequal loading of the gel). From these results we demonstrate the presence of two poly(A) sites for the *ura4* gene. The major poly(A) site is located in fragment D and a cryptic site in fragment E. The site determining element for the major poly(A) site is referred to as SDE1 and for the cryptic poly(A) site, SDE2.

Taking these results together it appears that fragment E plays an important role in mRNA 3′ end formation since it encodes signals which are necessary and sufficient for mRNA 3′ end formation. Furthermore, based on the RT-PCR experiments shown in Figure 2, transcription ceases to be detectable within fragment E. This non-coding region of the *ura4* gene was thus selected for further study.

Efficient mRNA 3′ end formation is directed by two sequence elements

A 3′ deletion series of fragment E from the *ura4* non-coding region was generated by *Bal*31 digestion. This created a set of fragments which were subcloned into the PUS vector (Figures 3A and 4A). The ability of each fragment to form mRNA 3′ termini was analysed by Northern blot analysis (Figure 4B). A single length transcript of ~750 nt is present corresponding to 100% 3′ end formation within the 260 nt E fragment (Figure 4B, lane 1), as previously described (Figure 3C, lane 6).

Single length transcripts are still detected in three *Bal*31 deletion clones; E:1−194, E1−170 and E:1−124 (Figure 3B, lanes 2, 3 and 4 respectively). However, deletion of a further 30 bp from the 3′ end of E:1−124 results in a sharp loss of 3′ end formation activity as determined by the appearance of a readthrough band of ~1100 nt (Figure 4B,

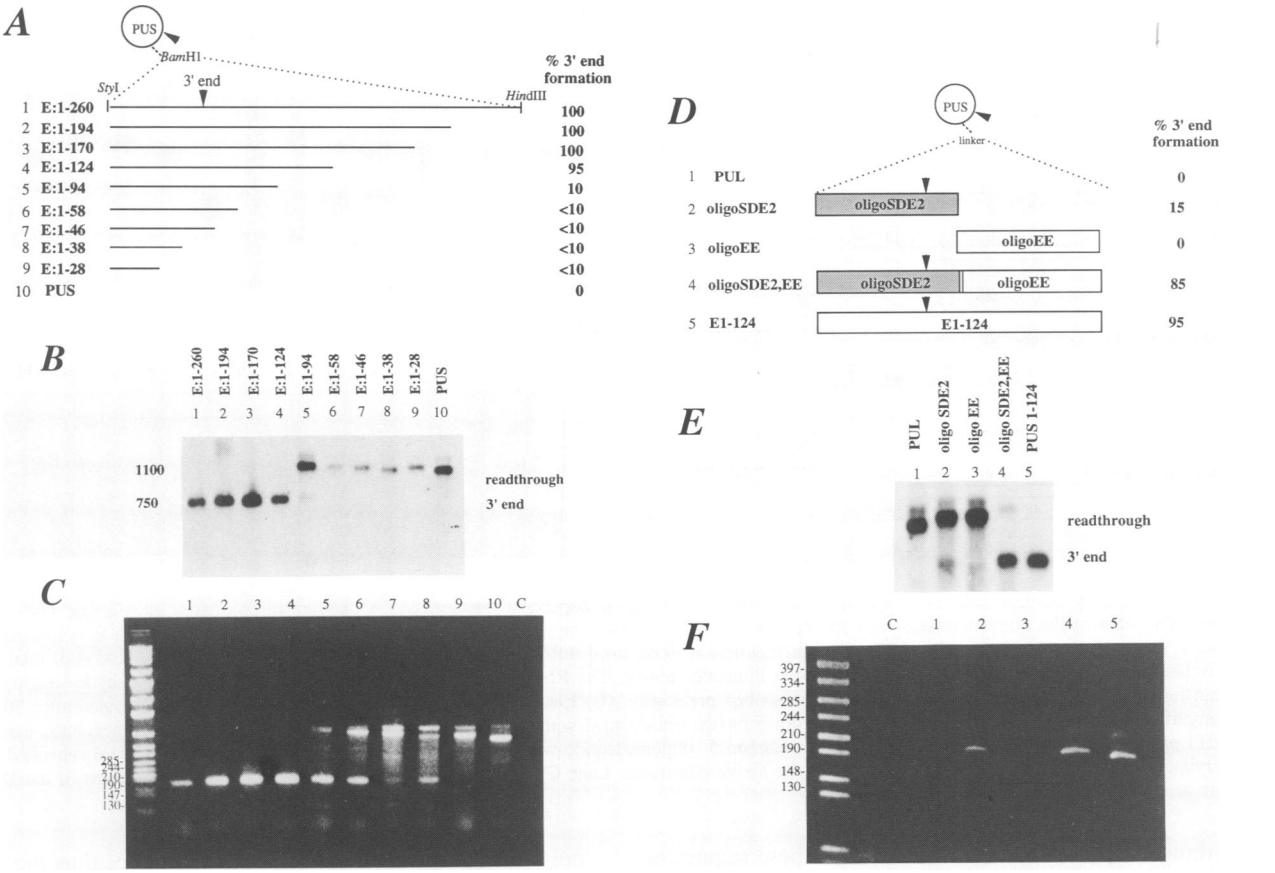

Fig. 4. Efficient mRNA 3′ end formation is directed by two sequence elements. (**A**) A diagram of deletion constructs transformed into *S.pombe*. The sizes of the *Bal*31 fragments are given. The polyadenylation site located within fragment E is illustrated by a black arrow. An estimation of the ability of each fragment to form *ura4* mRNA 3′ ends is also shown. (**B**) Northern hybridization of total RNA isolated from *S.pombe* transformed with constructs illustrated above. The RNA was separated on a 1.5% denaturing formaldehyde−agarose gel, transferred to a nylon membrane and hybridized to a 1.2 kb *Hin*cII−*Eco*RV random primer labelled DNA fragment of *ura4* to determine transcript lengths, which were compared with ethidium bromide stained RNA markers run in an adjacent lane. (**C**) Electrophoretic separation of RT-PCR products generated after 30 PCR amplification cycles, from total RNA isolated from *S.pombe* transformed with the above constructs (B). Reverse transcripts were generated using oligo(dT) primers (see Materials and methods) and a common 5′ oligonucleotide was used for each PCR. The RT-PCR products were separated on a 4% acrylamide gel. The lane numbers correspond to the constructs shown in (A). Lane C has no RNA added to the RT-PCR assay. The sizes of the smaller DNA markers are indicated. (**D**) A diagram of constructs transformed into *S.pombe*. The polyadenylation site located within fragment E is shown by a black arrow. An estimation of the ability of each fragment to form *ura4* mRNA 3′ ends is also shown. (**E**) Northern hybridization of total RNA isolated from *S.pombe* transformed with constructs shown in (D). The RNA was separated on a 1.5% denaturing formaldehyde−agarose gel, transferred to a nylon membrane and probed as above. (**F**) Electrophoretic separation of RT-PCR products generated after 30 PCR amplification cycles from total RNA isolated from *S.pombe* transformed with the above constructs (D). Lane C has no RNA added to the RT-PCR assay. Reverse transcripts were generated using oligo(dT) primers (see Materials and methods) and a common 5′ oligonucleotide was used for each PCR. The RT-PCR products were separated on a 4% acrylamide gel. The sizes of the DNA markers are indicated.

lane 5). Since nucleotides 1−94 of the E fragment still appear to produce the same length transcript as the entire E fragment, albeit at much reduced efficiency, it seems likely that sequences within this region define the site of 3′ end formation, whereas sequences between position nucleotide 94 and 124 are required for the efficient use of this site.

To determine whether the 3′ ends of transcripts from these constructs were formed at the same site, polyadenylated RNA was reverse transcribed using oligo(dT) primers with a C,G, or A nucleotide at their 3′ end to ensure that the primers can only hybridize to the poly(A) tail at the poly(A) site junction. These cDNAs were subsequently amplified by PCR, using the oligo(dT) primers and an oligonucleotide corresponding to the *ura4* gene sequence 87−64 bases upstream of the *Eco*RV site shown in Figures 1 and 2A. Such RT-PCR analysis results in a product of a defined length. As shown in Figure 4C, gel electrophoresis of the RT-PCR products gives a single band of ~190 bp in lanes 1−4 (E:1−260 to E:1−124). This PCR product (from E:1−260) was cloned and sequenced, and the poly(A) site within this fragment is shown in Figure 1, fragment E. This corresponds to the site predicted from the RT-PCR product length. Lanes 5−8 of Figure 4C give progressively more high molecular weight PCR products which presumably correspond to the readthrough transcripts observed in the Northern blot analysis (Figure 4B). The 190 bp PCR product is just visible for clones E:1−46 and E:1−38 (lanes 7 and 8).

These results indicate that polyadenylation occurs at or around the same distance downstream from sequences E:1−38. These nucleotides therefore contain signals which define the site of mRNA 3′ end formation. In contrast, the sequences near the poly(A) site would appear to be of little

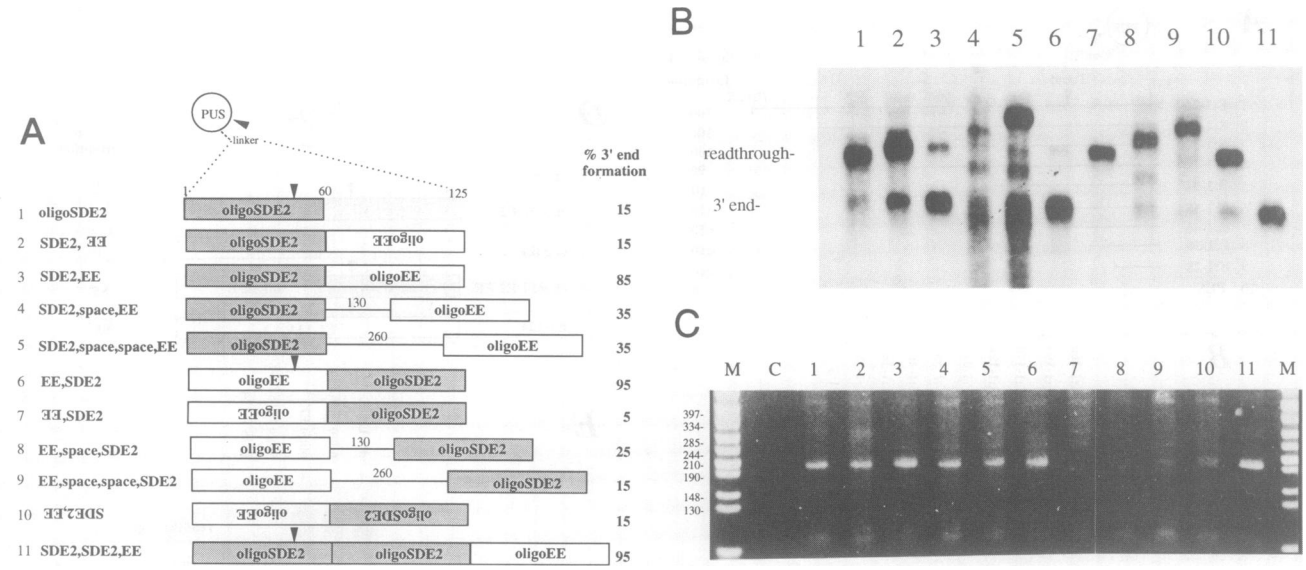

Fig. 5. The efficiency element behaves in a position-independent, orientation-dependent manner. (**A**) A diagram of constructs transformed into *S.pombe*. The sizes of the oligonucleotides and spacer fragments are shown. The major polyadenylation site located within fragment E is illustrated by a black arrow. An estimation of the ability of each fragment to form *ura4* mRNA 3′ ends is also shown. (**B**) Northern hybridization of total RNA isolated from *S.pombe* transformed with constructs illustrated above. The RNA was separated on a 1.5% denaturing formaldehyde–agarose gel, transferred to a nylon membrane and probed as described previously. (**C**) Electrophoretic separation of RT-PCR products generated after 30 PCR amplification cycles, from total RNA isolated from *S.pombe* transformed with the above constructs. Reverse transcripts were generated using oligo(dT) primers (see Materials and methods) and a common 5′ oligonucleotide was used for each PCR. The RT-PCR products were separated on a 4% acrylamide gel. The lane numbers correspond to the above constructs. Lane C has no RNA added to the RT-PCR assay. The sizes of the DNA markers are indicated.

importance in poly(A) site selection, since these sequences are substituted for polylinker in construct E:1–38. These findings contrast with those of Heidmann *et al.* (1992), where a PyAAA sequence appeared to be essential for poly(A) site selection in *S.cerevisiae*.

To test the hypothesis that efficient mRNA 3′ end formation within the E fragment is directed by two sequence elements, an oligonucleotide encoding nucleotides 7–61 of the E fragment (oligoSDE2) was tested for its ability to form *ura4* mRNA 3′ ends in the presence of a downstream oligonucleotide encoding sequences 61–124 (oligoEE, where EE stands for efficiency element). Oligos SDE2 and EE were inserted alone or in combination into a modified vector PUL which has a polylinker sequence inserted at the unique *Bam*HI site in the PUS vector (Figure 4D). The lengths of *ura4* transcripts produced by *S.pombe* transformed with these constructs (Figure 4D) were determined by Northern blot analysis (Figure 4E). These results demonstrate that when oligoEE is cloned downstream of oligoSDE2, mRNA 3′ end formation is restored to 85% compared with 95% for the first 124 bp of fragment E (compare Figure 4E, lanes 4 and 5). In contrast only 15% of the transcripts form termini in the presence of oligoSDE2 alone and only readthrough transcripts are detected when oligoEE is present downstream of the truncated *ura4* gene (Figure 4E, lanes 2 and 3). These results confirm the previous data that the first 60 bp of fragment E (oligoSDE2) encode a poly(A) site defining element and that sequences encoded within the second oligonucleotide (oligoEE) encode signals responsible for efficient utilization of the poly(A) site.

To determine the site of 3′ end formation of transcripts from these constructs, RT-PCR analysis was again performed using the *ura4*-specific and oligo(dT) primers described previously. The vector PUL contains extra polylinker sequences 5′ of the insertion site, thus the RT-PCR products from PUL SDE2 and PUL SDE2,EE are correspondingly longer than those from PUS1–124 (Figure 4F, lanes 2, 4 and 5). From these results we conclude that the sites of mRNA 3′ end formation are identical and that this downstream element contributes only to the efficiency of mRNA 3′ end formation. It is thus termed the efficiency element.

The efficiency element behaves in a position-independent, orientation-dependent manner

In order to determine the functional relationship between the site determining element and the efficiency element defined in the previous section, a variety of constructs were generated (see Figure 5A). Each construct was transformed into *S.pombe* and the subsequent lengths of the *ura4* transcripts determined by Northern blot analysis (Figure 5B). The corresponding site of polyadenylation was also determined by RT-PCR analysis (Figure 5C). We note that the RT-PCR signal of 210 nt correlated well with the Northern blot data for the *ura4* 3′ end signals.

Introduction of 130 or 260 bp of plasmid spacer DNA between the site determining element (oligoSDE2) and the efficiency element (oligoEE) resulted in a 50% decrease in mRNA 3′ end formation efficiency compared with oligoSDE2,EE (Figure 5A and B, lanes 3, 4 and 5). It should be noted, however, that this is still significantly more efficient than the site determining element alone and therefore these results demonstrate that the efficiency element can act in a distance-independent manner. The sites of polyadenylation are the same in each of these constructs (Figure 5C, lanes 3, 4 and 5). The additional readthrough bands visible in lanes 4 and 5 of Figure 4B presumably reflect the presence of other cryptic poly(A) sites in the spacer sequence.

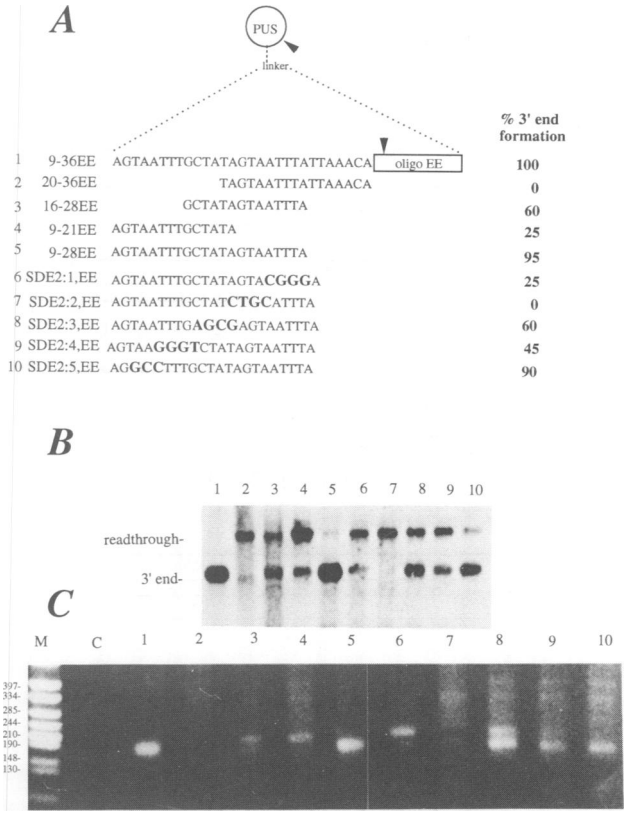

Fig. 6. Minimal sequence requirements of the site determining element. (**A**) A schematic diagram of constructs transformed into *S.pombe*. The sequences of the oligonucleotides are shown. The polyadenylation site is illustrated by a black arrow. An estimation of the ability of each fragment to form *ura4* mRNA 3′ ends is also shown. (**B**) Northern hybridization of total RNA isolated from *S.pombe* transformed with constructs illustrated above. The RNA was separated on a 1.5% denaturing formaldehyde–agarose gel, transferred to a nylon membrane and probed as described previously. (**C**) Electrophoretic separation of RT-PCR products generated after 30 PCR amplification cycles, from total RNA isolated from *S.pombe* transformed with the above constructs. Reverse transcripts were generated using oligo(dT) primers (see Materials and methods) and a common 5′ oligonucleotide was used for each PCR. The RT-PCR products were separated on a 4% acrylamide gel. The lane numbers correspond to the above constructs. Lane C has no RNA added to the RT-PCR assay. The sizes of the DNA markers are indicated.

When the efficiency element is positioned upstream of the site determining element highly efficient mRNA 3′ end formation is observed (Figure 5A and B, lanes 6 and 7) in the wild-type orientation only. However introduction of spacer elements between these two elements results in a substantial drop in 3′ end formation efficiency (Figure 5B, lanes 8 and 9). From the length of the RT-PCR product we infer that the site of polyadenylation is now located within the efficiency element in these constructs (Figure 5C, lane 6).

Constructs in which the orientation of the oligonucleotides is reversed, either individually (Figure 5A and B, lanes 2 and 7) or together (Figure 5A and B, lane 10) result in low efficiencies of mRNA 3′ end formation. Duplication of oligoSDE2 in the presence of oligoEE results in efficient 3′ end formation (Figure 5A and B, lane 11). Again, from the length of the RT-PCR product we infer that the site of 3′ end formation is located within the 5′ oligoSDE2 (Figure 5C, lane 11).

These results demonstrate that the efficiency element behaves in a position-independent, orientation-dependent manner.

Minimal sequence requirements for efficient 3′ end formation of ura4 transcripts

In order to define the precise sequence requirements within both the site determining element and the efficiency element, deletions and mutations were introduced into both elements as shown in Figures 6A and 7A. These constructs were transformed into *S.pombe* and their ability to form mRNA 3′ ends was determined by Northern blot analysis (Figure 6B and 7B).

Deletion of both 5′ and 3′ sequences of oligo SDE2 revealed that the site determining element lies within nucleotides 9–36 of oligoSDE2, since when this region is positioned upstream of oligoEE (9-36EE) extremely efficient mRNA 3′ end formation is observed (Figure 6B, lane 1). Further deletion studies reveal nucleotides 9–28 still encode the site determining element since when this region is placed upstream of oligoEE (9-28EE) extremely efficient mRNA 3′ end formation is still observed (Figure 6B, lane 5), compared with 20-36EE, 16-28EE and 9-21EE (Figure 6B, lanes 2, 3 and 4). Mutations within nucleotides 9–28 all have deleterious effects on mRNA 3′ end formation efficiency, (Figure 6B, lanes 6–10). Although substitution of the 5′ TAA to GCC had little effect (Figure 6B, lane 10), substitution of the second AGTA motif resulted in complete inhibition of mRNA 3′ end formation (Figure 6B, lane 7). From these experiments we find that the sequence TTTGCTATAGTAATTT plays a central role in determining the site and efficiency of mRNA 3′ end formation in *S.pombe*.

RT-PCR analysis of the transcripts generated from these constructs (Figure 6C) confirms the Northern blot analysis. However, it is interesting to note that the mutations causing a reduction in *ura4* mRNA 3′ end formation also appear to have an altered site of polyadenylation ~20 nt downstream. For example constructs 9-21EE and E:1EE have substantially weakened site determining elements (25% 3′ end formation) and give the larger PCR product (Figure 6C, lanes 4 and 6). Similarly constructs 16-28EE and SDE2:3,EE have more efficient site determining elements (60% 3′ end formation) and so give both PCR products. These findings are entirely consistent with the role of oligoSDE2 as a site determining element.

To determine which signals are required for the 3′ end formation efficiency element, a *Nco*I site was introduced in the middle of the 60 bp oligoEE, encoding the efficiency element. This *Nco*I-oligoEE oligonucleotide and both of the halves produced following restriction with *Nco*I were tested for their effect on efficiency of mRNA 3′ end formation by cloning *Nco*I-oligoEE before or after digestion, downstream of the site determining element, oligoSDE2 (Figure 7A, constructs 2, 3 and 4). Northern blot analysis demonstrates that the sequences responsible for efficient mRNA 3′ end formation reside in the 3′ half of oligoEE, where, in contrast with the 5′ EE fragment very little readthrough is observed (compare Figure 7B, lanes 3 and 4). Substitution mutations of the first eight and last six nucleotides of the 3′ EE region have little effect on the efficiency of mRNA 3′ end formation (Figure 7A and B, lane 6 and 10). Substitution mutations within the rest of this region were found to be deleterious

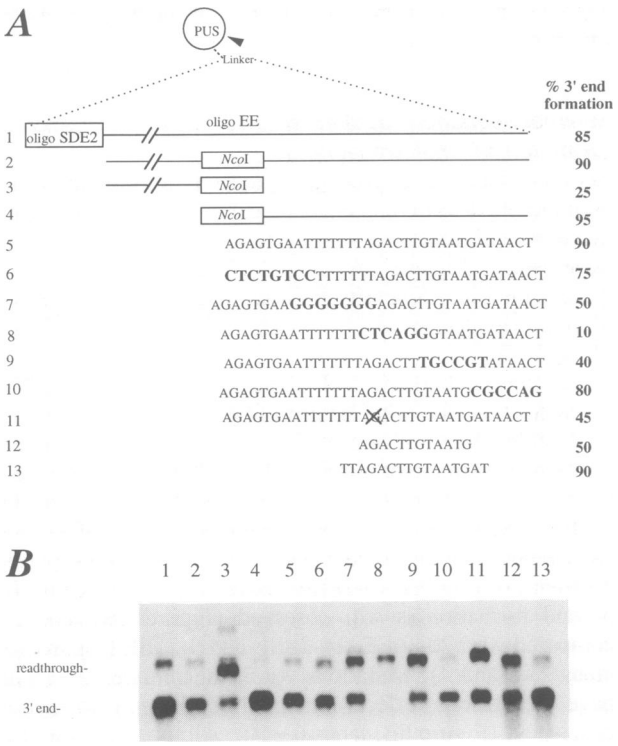

Fig. 7. Minimal sequence requirements of the efficiency element. (**A**) A schematic diagram of constructs transformed into *S.pombe*. The sequences of the oligonucleotides are shown. An estimation of the ability of each construct to form *ura4* mRNA 3′ ends is also shown. (**B**) Northern hybridization of total RNA isolated from *S.pombe* transformed with constructs illustrated above. The RNA was separated on a 1.5% denaturing formaldehyde–agarose gel, transferred to a nylon membrane and probed as described previously.

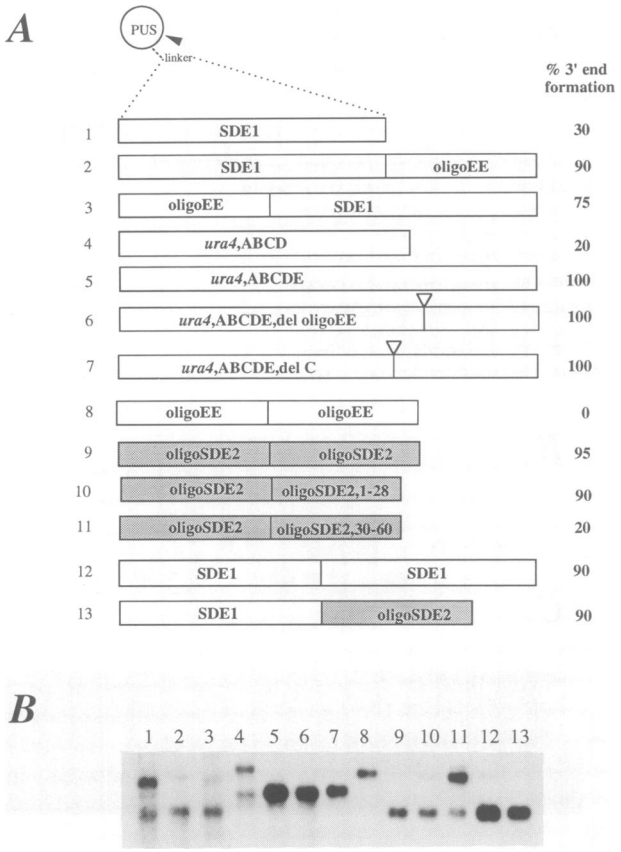

Fig. 8. Two site determining elements are sufficient for efficient mRNA 3′ end formation. (**A**) A schematic diagram of constructs transformed into *S.pombe*. Triangles above the constructs denote sites from which deletions were made (see text). Constructs 4–7 use the PUS rather than PUL vector. An estimation of the ability of each construct to form *ura4* mRNA 3′ ends is also shown. (**B**) Northern hybridization of total RNA isolated from *S.pombe* transformed with constructs illustrated above. The RNA was separated on a 1.5% denaturing formaldehyde–agarose gel, transferred to a nylon membrane and probed as described previously.

(Figure 7A and B, lanes 7–9) and therefore play an important role in efficient mRNA 3′ end formation. The importance of this region is supported by the striking affect of the deletion of a single base which reduces 3′ end formation by 45% (Figure 7A and B, lane 11). When a 16 bp oligonucleotide containing part of this region was placed downstream of oligoSDE2, efficient mRNA 3′ end formation was restored (Figure 7A and B, lane 13). In contrast, a 12 bp oligonucleotide did not restore full mRNA 3′ end formation efficiency (Figure 7A and B, lane 12).

These results demonstrate that the sequence TTAGACTTGTAATGAT is sufficient to restore the efficiency of mRNA 3′ end formation of oligoSDE2. Intriguingly, this sequence is located directly downstream of the last oligonucleotide with which *ura4* transcripts could be detected by RT-PCR (see Figures 1 and 2C, lanes 6 and 7).

Two site determining elements are sufficient for efficient mRNA 3′ end formation

To test whether the efficiency box located within oligoEE of the *Sty*I–*Hin*dIII E fragment contributes to the efficiency of the major *ura4* poly(A) site, a construct was generated in which oligoEE (containing the efficiency box) was cloned downstream of fragment BCD also called SDE1, which contains the major poly(A) site located in fragment D (Figure 1). SDE1 forms mRNA 3′ ends inefficiently when cloned into the PUL vector (Figure 3C, lane 5 and Figure 8B, lane 1) and thus behaves in a similar fashion to oligoSDE2. In contrast, when oligoEE is cloned either downstream (Figure 8B, lane 2) or upstream (Figure 8B, lane 3) of SDE1, the efficiency of mRNA 3′ end formation is significantly increased. This demonstrates that the efficiency element in oligoEE works well on both different site determining elements. Furthermore, this implies that the efficiency element in fragment E is contributing to the overall process of mRNA 3′ end formation within fragment D and explains the reduction in mRNA 3′ end processing observed when fragment E is deleted from the otherwise intact *ura4* 3′ end sequence.

As expected when fragment C was precisely deleted from the *S.pombe ura4* gene we observe that 3′ end formation switches to the more distal poly(A) site in oligoSDE2 as shown in Figure 8B (compare lanes 5 and 7). Since deletion of C will reduce the size of the *ura4* transcript by 35 nt, the fact that the band in lane 7 is slightly larger than that in lane 5 is especially significant. This observation has been confirmed by RT-PCR (data not shown). However, when the efficiency sequence TTAGACTTGTAATGAT was mutated in the *S.pombe ura4* gene (see Materials and methods), no effect on *ura4* mRNA 3′ end formation was observed either in Northern blots (Figure 8, compare lanes

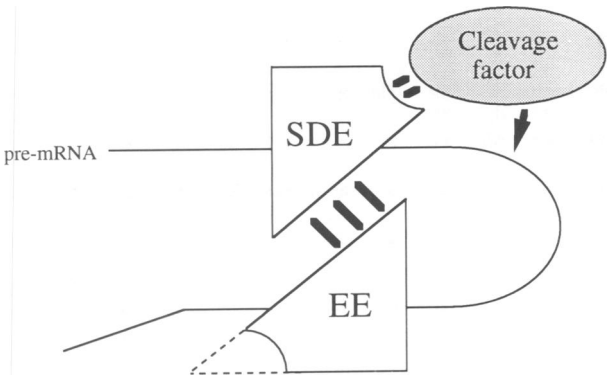

Fig. 9. Model for the mechanism of 3′ end formation in the *S.pombe ura4* gene. Diagram depicts factors interacting with the site determining and efficiency elements of the *ura4* pre-mRNA The dotted line that completes the triangle for the EE factor(s) signifies that this factor can either be the same as the SDE factor or specific to EE. The binding of factor(s) to EE enhances binding of factor(s) to SDE which in turn interacts with cleavage factor to promote *ura4* 3′ end formation.

4, 5 and 6) or by RT-PCR analysis (data not shown). This indicates that another region within fragment E contributes to efficient mRNA 3′ end formation. We therefore tested the ability of SDE2 in fragment E to contribute to the efficiency of mRNA 3′ end formation. This was first performed by analysing RNA from *S.pombe* transformed with oligoSDE2 cloned downstream of SDE1 (Figure 8B, lane 13). This was indeed found to restore efficient mRNA 3′ end formation. Since SDE1 has similar properties to SDE2 in fragment E, it was replaced by another oligoSDE2 to test whether two identical site determining elements (oligoSDE2,oligoSDE2) could function efficiently to form mRNA 3′ ends. As shown in Figure 8A (lane 9) this is also the case (Figure 8A and B, lane 9). In contrast, when two efficiency elements are placed in tandem (construct oligoEE,oligoEE) no 3′ end formation was observed (Figure 8A and B, lane 8).

To prove further that it was the site determining element within oligoSDE2 which contributes to 3′ end formation efficiency, nucleotides 1−28, which more precisely contain the site determining element, were cloned downstream of oligoSDE2. Again it was found that these sequences do contribute to efficient mRNA 3′ end formation by oligoSDE2 (Figure 8A and B, lane 10). In contrast the second half of oligoSDE2 (30−60) only slightly enhanced mRNA 3′ end formation efficiency by oligoSDE2 (Figure 8A and B, lane 11). These results indicate that two site determining elements are sufficient for mRNA 3′ end formation. A prediction of this result might be that efficient mRNA 3′ end formation could be obtained by duplication of the site determining element within the BCD fragment (SDE1) and again this is found to be so (Figure 8B, lane 12). Thus it seems reasonable that the deletion of the efficiency element in fragment E had no effect *in vivo* because this deletion was compensated by the presence of SDE2.

Discussion

The results presented in these studies describe a series of experiments designed to identify the signals required for RNA 3′ end formation in the *ura4* gene of *S.pombe*. We first establish the extent of transcription past the gene's poly(A) site using a highly sensitive RT-PCR approach. We find that RNA transcripts are detectable at significant levels immediately following the poly(A) site but that these transcripts become undetectable 120 bp downstream. This same procedure has been previously employed to define the region of transcriptional termination for the human $\alpha 2$ globin gene and was found to be in close agreement with data obtained by nuclear run-off analysis (Owczarek *et al.*, 1992). From these considerations it seems plausible that termination of transcription in the *ura4* gene occurs ~120 nt downstream of the major *ura4* poly(A) site, coincident with the position of the efficiency element. These observations are clearly consistent with the notion that there may be tight linkage between polyadenylation and termination in yeast

We next identified two RNA 3′ end formation signals within this downstream region, one which acts as a site determining element for polyadenylation (oligoSDE2) and another which is required for efficient utilization of this polyadenylation site (oligoEE). These elements in combination are sufficient for 3′ end formation of *ura4* mRNA. We further characterize the interaction of these two elements and show that the efficiency element behaves in a position-independent, orientation-dependent manner, but cannot form 3′ ends independently of the site determining element. These results demonstrate that production of mRNA 3′ termini in *S.pombe* involves at least two functionally distinct elements: a site determining element (SDE) and an enhancing or efficiency element (EE), working in concert. However, we note that when the efficiency element is positioned upstream of the site determining element, the 3′ ends of transcripts are located within the efficiency element, which argues that it too can function as a site determining element in this context (Figure 5, see oligoEE,SDE2). Furthermore, this efficiency element can be functionally replaced by a second copy of the site determining element (Figure 8, see construct oligoSDE2,oligoSDE2). This site determining element can also be coupled to the major site determining element of the *ura4* gene encoded within fragment BCD, resulting in an efficiently recognized 3′ end formation signal (Figure 8, see construct SDE1,oligoSDE2). When testing the prediction that two site determining elements are sufficient for efficient 3′ end formation, we found that duplicating either SDE1 or SDE2 results in efficient 3′ end formation (see Figure 8). Thus although 3′ end formation of *ura4* mRNA in *S.pombe* requires two functionally distinct elements working in concert, we demonstrate that the same sequence element can perform both distinct functions. In summary, the minimal sequence requirements for efficient *ura4* mRNA 3′ end formation in *S.pombe* comprise either two site determining elements or one site determining element combined with an efficiency element.

Figure 9 presents a working model for the arrangement of the bipartite poly(A) signal of the *S.pombe ura4* gene. As indicated a factor binding to SDE is predicted to interact with the cleavage/polyadenylation factor (or factors) which then promotes cleavage and polyadenylation downstream. However, the factor that interacts with SDE is further stabilized by interaction with a second factor which binds to the EE RNA sequence. As EE may be replaced by a second copy of SDE it is also possible that the factor

interacting with EE is a second SDE binding factor. This speculative model is consistent with all of the sequence and positional parameters defined in these studies for SDE and EE. In particular both elements can work at various distances (albeit at variable efficiency) and are entirely orientation-dependent.

These findings raise a number of interesting questions. First, what sequences comprise the site determining element? Computational analysis of the 3′ ends of *S.pombe* genes has not revealed any sequence homologies (Humphrey *et al.*, 1991). Furthermore, the minimal SDE2 sequence TTTGCTATAGTAATTT shares no obvious homology with sequences within BCD, which also contains a site determining element (SDE1). This 16 nt element does, however, show some sequence similarities to the RNA 3′ end signals UAG...UAUGUA and UAUAUA from the distantly related budding yeast (Russo *et al.*, 1991; Iringer and Braus, 1994). More encouragingly, this element encodes a region of homology close to the sequence UAUAGUUA, recently proposed to be required for *in vitro* polyadenylation of the *S.cerevisiae* cyc1 mRNA (S.-Y.Wu and T.Platt, personal communication). However this sequence is not generally found in *S.cerevisiae* 3′ ends and is also not evident within the *ura4* region BCD.

It will be of interest to establish the evolutionary relationship of this bipartite poly(A) signal to lower and higher eukaryotes. We have previously demonstrated that an *S.cerevisiae* poly(A) signal for the *CYC1* gene functions in *S.pombe* while mammalian poly(A) signals do not. These results suggest that the actual nucleotide sequence signals for polyadenylation may be more homologous between *S.pombe* and *S.cerevisiae* than with mammals. However, the bipartite arrangement of the SDE and E elements in the *ura4* gene is very reminiscent of mammalian poly(A) signals where two sequence elements, the hexanucleotide AAUAAA and a U- or GU-rich downstream signal are necessary for efficient 3′ end formation (Proudfoot, 1991). Recently many of the factors that interact with mammalian poly(A) signals have been characterized [for review see Wahle and Keller (1992)]. The cleavage polyadenylation stimulation factor (CPSF) that interacts with AAUAAA may be analogous to the factor binding to SDE while the cleavage stimulation factor (CStF) may correspond to the factor binding to EE and the SDE binding factor (see Figure 9). Further genetic and biochemical analysis will be required to establish a complete understanding of RNA 3′ end formation in *S.pombe* and how this relates to other eukaryotes.

Materials and methods

DNA constructions

PUS and PUL plasmid constructs. Plasmid PUS, encodes the *Hin*dIII−*Eco*RV fragment of the *S.pombe ura4* gene inserted into the *Sma*I site of Pirt2 as previously described. A unique *Bam*HI site is positioned immediately adjacent to the 3′ end of the *ura4* insert (at the *Eco*RV site) into which the various *ura4* 3′ non-coding region fragments were inserted by blunt-ended ligation (Humphrey *et al.*, 1991).

Plasmid PUL was constructed by synthesizing the 35 bp polylinker:

*Xho*I *Nhe*I *Bgl*II *Not*I *Bam*HI
CTCGAGGCTAGCAGATCTGCGGCCGCGGATCC

and inserting it into the *Bam*HI site of PUS. OligoSDE2 and derivatives of it, were constructed by synthesizing oligonucleotides with 5′ overhangs compatible with *Nhe*I and *Bgl*II restriction sites. After annealing, these oligonucleotide pairs were directionally cloned into PUL vector restricted with *Nhe*I and *Bgl*II. A similar approach was utilized for oligoEE but in this case 5′ overhangs compatible with *Bgl*II and *Not*I were employed. Oligonucleotides cloned into alternative sites in the polylinker were blunt-ended with Klenow prior to ligation, as was *Nco*I-oligoEE. The 100 bp BCD fragment and the 130 bp spacer fragment (produced through restriction of pGEM with *Hae*III) were also inserted into blunt-ended sites in the PUL polylinker. All clones were sequenced before being transformed into *S.pombe*.

Bal31 deletion series. PUS E was digested with *Hin*dIII and then subjected to *Bal*31 digestion. The *LEU2* gene was then reintroduced as a 2.2 kb *Hin*dIII fragment into each construct in the same orientation as found in PUS. All clones were sequenced before being transformed into *S.pombe*.

PUSA-E deletions of C and DS (del C and del oligoEE). Del C was constructed by excising fragment C from PUS A−E with *Sca*I and *Ssp*I. Del oligoEE was constructed using PCR mutagenesis. DNA primers were synthesized that prime just outside and away from the efficiency element located in oligoEE. These primers in conjunction with a primer either in the 5′ *ura4* coding sequence or 3′ *LEU2* sequence were used to amplify sequences on either side of the efficiency element in oligo DS. These two PCR products were then recut with *Avr*II (*Avr*II recognizes the *Sty*I site at the 3′ end of fragment A) or *Hin*dIII and reinserted into *Avr*II + *Hin*dIII cut PUS A−E. These manipulations substituted AGACTTGTAAT of the efficiency element with a linker sequence CCCCTGGGG.

S.pombe RNA analysis

S.pombe was transformed as described using the LiCl method described by Bröker (1987) and total RNA was isolated according to the 'hot phenol' method of Kohrer and Domdey (1991).

Northern blot analysis. For Northern hybridizations, 30 μg of total RNA were separated on a denaturing formaldehyde gel according to the method of Rave *et al.* (1979). After transfer onto Hybond-N (Amersham) the bound RNA was hybridized to a 1.2 kb *Hin*cII−*Eco*RV DNA fragment of *S.pombe ura4*, or a 2.2 kb *Hin*dIII fragment of *S.cerevisiae LEU2* which was random primer labelled as described in Feinberg and Vogelstein (1984). The size of hybridizing bands was determined by comparison with RNA size markers (0.16−1.77 kb) obtained from Gibco-BRL. Quantitation of the Northern blot data was carried out by laser densitometry of several radioautographs. Percentage 3′ end formation was calculated as the percentage of the smaller *ura4* 3′ end band to the total amount of RNA specific for the *ura4* probe (ie the sum of the *ura4* 3′ end and readthrough bands).

Reverse transcription and PCR analysis (RT-PCR). Total RNA from *S.pombe* was reverse transcribed as described by Innis *et al.* (1990), using oligo(dT) oligonucleotides of the sequence (5′)TGCATGCGGCCGTTTTTTTTT-TTTTTG/A/C(3′), 1 μg of total *S.pombe* RNA was reverse transcribed in the presence of 10 mM Tris−HCl (pH 8.3), 50 mM KCl, 0.001% gelatin, 1 mM dNTPs (Boerhinger Mannheim), 5 mM $MgCl_2$, 1 unit of reverse transcriptase AMV (Life Sciences Inc), oligonucleotide primer (2.5 pmol), 10 units RNasin (Promega Biotec) and incubated at 42°C for 45 min, then 52°C for 30 min. Reverse transcriptase was inactivated by heating at 95°C for 10 min. About 50 ng of reverse transcribed *S.pombe* cDNA products were then PCR amplified according to the protocol of Innis *et al.* (1990), by adding cDNA from the reverse transcription reaction to a PCR mixture containing 0.2 mM dNTPs, 2 mM $MgCl_2$, 1 unit of Taq polymerase (Cetus) and 0.5 pmol of a *ura4*-specific primer and each of oligo(dT) primers described above. This reaction mix was covered by a layer of paraffin to prevent evaporation and then thermally cycled to 95°C for 1 min, 64°C for 1 min, 72°C for 3 min, for 30 cycles using a Perkin Elmer−Cetus PCR machine.

Various RT-PCR products were cloned into the *Sma*I site of pGEM7ZF$^+$ and subsequently sequenced in both directions so as to determine the position of 3′ end formation.

The quantitative RT-PCR (data presented in Figure 2) was carried out as follows. cDNA was generated as above, but using PUS A−E transformed *S.pombe* RNA or synthetic *ura4* RNA (see below) and the 10 different primers indicated in Figures 1 and 2A. These cDNAs were then amplified (either 20 or 30 cycles) using a common 5′ ^{32}P labelled primer (sense sequence to nucleotides 1125−1148 of the *ura4* gene sequence; Grimm *et al.*, 1988) and each of the 10 3′ primers originally used to make the cDNA. The RT-PCR products shown in Figure 2B were excised from an ethidium bromide stained gel and the radioactivity in each band was determined by Cerenkov counting. The results presented in Figure 2A are an average of four separate experiments. The control synthetic *ura4* RNA was generated by T7 transcription of pGEM 7Zf plasmid with the *ura4 Eco*RV−*Hin*dIII fragment inserted into the plasmid's polylinker sequence. A further spacer fragment of 130 bp (from pGEM) was inserted into the *Avr*II site of the *ura4* sequence to allow the synthetic RNA PCR products to be distinguished from the *S.pombe* products.

Many of these manipulations have been described in greater detail by Owczarek *et al.* (1992).

Acknowledgements

We are grateful to members of the N.J.P. and P.Nurse labs for advice and encouragement throughout these studies. T.H. and C.E.B. were both supported by a Programme Grant from the Wellcome Trust to N.J.P. (No. 032773).

References

Abe,A., Hiraoka,Y. and Fukusawa,T. (1990) *EMBO J.*, **9**, 3691–3697.
Bröker,M. (1987) *Biotechniques*, **5**, 516–518.
Butler,J.S. and Platt,T. (1988) *Science*, **242**, 1270–1274.
Butler,J.S., Sadhale,P. and Platt,T. (1990) *Mol. Cell. Biol.*, **10**, 2599–2605.
Chen,J. and Moore,C. (1992) *Mol. Cell. Biol.*, **12**, 3470–3481.
Feinberg,A.P. and Vogelstein,B. (1984) *Anal. Biochem.*, **137**, 266–267.
Girard,J., Feliu,J., Caizergues-Ferrer,M. and Lapeyre,B. (1993) *Nucleic Acids Res.*, **21**, 1881–1887.
Grimm,C., Kohli,J., Murray,J. and Maundrell,K. (1988) *Mol. Gen. Genet.*, **215**, 81–86.
Heidmann,S., Obermaier,B., Vogel,K. and Domdey,H. (1992) *Mol. Cell. Biol.*, **12**, 4215–4229.
Henikoff,S., Kelly,J.D. and Cohen,E.H. (1983) *Cell*, **33**, 607–614.
Humphrey,T., Sadhale,P., Platt,T. and Proudfoot,N.J. (1991) *EMBO J.*, **10**, 3503–3511.
Hyman,L.E. and Moore,C.L. (1993) *Mol. Cell. Biol.*, **13**, 5159–5167.
Hyman,L.E., Seiler,S.H., Whorisky,J. and Moore,C.L. (1991) *Mol. Cell. Biol.*, **11**, 2004–2012.
Innis,M.A., Gelfand,D.H., Sninsky,J.J. and White,T.J. (1990) *PCR Protocols. A Guide to Methods and Applications*. Academic Press, San Diego, California.
Irniger,S. and Braus,G. (1994) *Proc. Natl Acad. Sci. USA*, **91**, 257–261.
Irniger,S., Egli,C.M. and Braus,G. (1991) *Mol. Cell. Biol.*, **11**, 3060–3069.
Kohrer,K. and Domdey,H. (1991) *Methods Enzymol.*, **194**, 398–401.
Lingner,J., Radke,I., Wahle,E. and Keller,W. (1991a) *J. Biol. Chem.*, **14**, 8742–8746.
Lingner,J., Kellermann,J. and Keller,W. (1991b) *Nature*, **354**, 496–498.
Osborne,B.I. and Guarente,L. (1988) *Genes Dev.*, **2**, 766–772.
Osborne,B.I. and Guarente,L. (1989) *Proc. Natl Acad. Sci. USA*, **86**, 4097–4101.
Owczarek,C.M., Enriquez-Harris,P. and Proudfoot,N.J. (1992) *Nucleic Acids Res.*, **20**, 851–858.
Proudfoot,N.J. (1989) *Trends. Biochem. Sci.*, **14**, 105–110.
Proudfoot,N.J. (1991) *Cell*, **64**, 671–674.
Rave,N., Crkvenjaker,R. and Boedtker,X. (1979) *Nucleic Acids Res.*, **6**, 3559–3567.
Ruohola,H., Baker,S.M., Parker,R. and Platt,T. (1988) *Proc. Natl Acad. Sci. USA*, **85**, 5041–5045.
Russo,P. and Sherman,F. (1989) *Proc. Natl Acad. Sci. USA*, **86**, 8348–8352.
Russo,P., Li,W.-Z., Hampsey,D.M., Zaret,K.S. and Sherman,F. (1991) *EMBO J.*, **10**, 563–571.
Russo,P., Li,W.-Z., Guo,Z. and Sherman,F. (1993) *Mol. Cell. Biol.*, **13**, 7835–7849.
Sadhale,P. and Platt,T. (1992) *Mol. Cell. Biol.*, **12**, 4262–4270.
Sadhale,P.P., Sapolsky,R., Davis,R.W., Butler,J.S. and Platt,T. (1991) *Nucleic Acids Res.*, **19**, 3683–3688.
Wahle,E. and Keller,W. (1992) *Annu. Rev. Biochem.*, **61**, 419–440.
Wu,S.-Y. and Platt,T. (1993) *Proc. Natl Acad. Sci. USA*, **90**, 6606–6610.
Zaret,K.S. and Sherman,F. (1982) *Cell*, **28**, 563–573.
Zaret,K.S. and Sherman,F. (1984) *J. Mol. Biol.*, **176**, 107–135.

Received on January 24, 1994; revised on March 18, 1994